AFOSR Final Technical Report

AFOSR-TR-

NOISE SUPPRESSION IN JET INLETS

Prepared for

Air Force Office of Scientific Research
Director of Aerospace Sciences

Bolling AFB, D.C.

by

Ben T. Zinn

William L. Meyer

Brady R. Daniel

School of Aerospace Engineering
Georgia Institute of Technology
Atlanta, Georgia 30332

Approved for public release; distribution unlimited

AFOSR Contract No. F49620-77-C-0066 February 1980

SECURITY CLASSIFICATION OF THIS PAGE *(When Data Entered)*

REPORT DOCUMENTATION PAGE

READ INSTRUCTIONS BEFORE COMPLETING FORM

1. REPORT NUMBER: AFOSR-TR-	2. GOVT ACCESSION NO.
3. RECIPIENT'S CATALOG NUMBER	
4. TITLE *(and Subtitle)*: Noise Suppression in Jet Inlets	5. TYPE OF REPORT & PERIOD COVERED: Final, Feb. 1, 1979 - Jan. 31, 1980
	6. PERFORMING ORG. REPORT NUMBER
7. AUTHOR(s): Ben T. Zinn, William L. Meyer, Brady R. Daniel	8. CONTRACT OR GRANT NUMBER(s): AFOSR-F49620-77-C-0066
9. PERFORMING ORGANIZATION NAME AND ADDRESS: School of Aerospace Engineering, Georgia Institute of Technology, Atlanta, Ga. 30332	10. PROGRAM ELEMENT, PROJECT, TASK AREA & WORK UNIT NUMBERS
11. CONTROLLING OFFICE NAME AND ADDRESS: Air Force Office of Scientific Research, Director of Aerospace Studies, Bolling AFB, DC	12. REPORT DATE: February 1980
	13. NUMBER OF PAGES
14. MONITORING AGENCY NAME & ADDRESS *(if different from Controlling Office)*	15. SECURITY CLASS. *(of this report)*
	15a. DECLASSIFICATION/DOWNGRADING SCHEDULE: Unclassified

16. DISTRIBUTION STATEMENT *(of this Report)*

Approved for Public Release; Distribution Unlimited

17. DISTRIBUTION STATEMENT *(of the abstract entered in Block 20, if different from Report)*

18. SUPPLEMENTARY NOTES

19. KEY WORDS *(Continue on reverse side if necessary and identify by block number)*

Acoustic Radiation
Duct Acoustics
Jet Propulsion Noise
Aircraft Noise

20. ABSTRACT *(Continue on reverse side if necessary and identify by block number)*

This report summarizes the work performed in the third and last year of an AFOSR sponsored research program (AFOSR Contract No. F49620-77-C-0066). This research program was concerned with the development of an analytical technique, based on an integral representation of the external solutions of the Helmholtz equation, for the prediction of the sound radiated from complicated, acoustically lined, axisymmetric bodies having complex sound sources. The purpose of this research program was to generate

DD FORM 1 JAN 73 1473

SECURITY CLASSIFICATION OF THIS PAGE *(When Data Entered)*

efficient computer codes for the prediction of the sound radiated from acoustically lined jet engine inlets. During the first two years of work under this contract the above goals were accomplished and are documented in the previous two AFOSR ANNUAL TECHNICAL REPORTS numbered AFOSR-TR-78-0696 and AFOSR-TR-79-0614.

This report is concerned with the progress made during the third year of this contract when experimental tests were run on various configurations for comparison with and verification of the results obtained from the axisymmetric computer codes which model the integral technique. In the experimental tests two geometrical configurations were studied, a straight duct and a jet engine inlet. Both of these configurations were tested with hard walls and the straight duct was tested with an acoustic liner consisting of a matrix of Helmholtz resonators. It was found that very good agreement was obtained for the hard walled configurations while there were some discrepancies with the lined wall case. It is conjectured that this discrepancy in some of the lined wall results is mainly due to the particular liner theory used to calculate the effective admittance of the liner.

Abstract

This report summarizes the work performed in the third and last year of an AFOSR sponsored research program (AFOSR Contract No. F49620-77-C-0066). This research program was concerned with the development of an analytical technique, based on an integral representation of the external solutions of the Helmholtz equation, for the prediction of the sound radiated from complicated, acoustically lined, axisymmetric bodies having complex sound sources. The purpose of this research program was to generate efficient computer codes for the prediction of the sound radiated from acoustically lined jet engine inlets. During the first two years of work under this contract the above goals were accomplished and are documented in the previous two AFOSR ANNUAL TECHNICAL REPORTS numbered AFOSR-TR-78-0696 and AFOSR-TR-79-0614.

This report is concerned with the progress made during the third year of this contract when experimental tests were run on various configurations for comparison with and verification of the results obtained from the axisymmetric computer codes which model the integral technique. In the experimental tests two geometrical configurations were studied, a straight duct and a jet engine inlet. Both of these configurations were tested with hard walls and the straight duct was tested with an acoustic liner consisting of a matrix of Helmholtz resonators. It was found that very good agreement was obtained for the hard walled configurations while there were some discrepancies with the lined wall case. It is conjectured that this discrepancy in some of the lined wall results is mainly due to the particular liner theory used to calculate the effective admittance of the liner.

Introduction

This report summarizes the results obtained during the third year of support under AFOSR contract number F49620-77-C-0066. This contract was initiated February 1, 1977 and the results obtained during the first two years of support are contained in AFOSR technical reports AFOSR-TR-78-0696 and AFOSR-TR-79-0614.

The main objective of the research program conducted under this contract was to develop an analytical technique, both the theory and associated computer codes, for predicting the sound field radiated from axisymmetric jet engine inlet configurations with lined walls and to compare some analytical predictions with the results of experimental tests. The development of the theory, which is based on a special integral representation of the external solutions of the Helmholtz equation, was motivated by the need for an analytical approach that could be used to predict the effects of sound source modifications and acoustic liners on the sound field radiated from an inlet without having to resort to costly, full scale experimental testing. During the first two years of this contract the axisymmetric formulation of the integral solution technique[1,3] was developed along with two efficient, general computer programs; one to solve for the surface distributions of the acoustic quantities of interest and the other to solve for the distributions of the acoustic quantities in the field surrounding the body.

During the third contract year sound radiation experiments were performed with two geometrically different configurations, a straight duct and the QCSEE jet engine inlet of Ref. (4), for comparison with analytical

results for the same bodies. The straight duct configuration was tested with both a hard and a soft wall while the inlet configuration was only tested with a hard wall. Tasks performed during the third contract year included:

A.) Calibration of the anechoic chamber

This was necessary to find out how well the anechoic chamber approximated the results that would be gotten if true free field measurements could be made. These calibrations were done with all of the support apparatus for the test bodies and the microphones in place so as to get an idea of the magnitude of the errors involved.

B.) Set-up of the electronic equipment

This task was not as straight forward as it might seem as it was found that in order to get relatively stable amplitude and phase measurements it was necessary to pre-condition the signals coming from the microphones through the use of both high and low pass filters. Since all of the signals were passed through the same filters, including the reference signal from the reference microphone, any phase or amplitude shift caused by the filters could be subtracted out.

C.) Conduct of the experiments

Each of the experimental tests were run at least twice on two different days and the results of these separate tests were compared. This was necessary to get an estimate of the repeatability of the experimental data. It was also used as a check on the validity of the data as the data was read directly from meters and transcribed by hand as no on line data acquisition system was available for use on this project.

D.) Prediction of the tested liner admittance

A liner was designed and fabricated for the lined straight duct tests. To do this design the theory of Garrison[5] was employed. The liner thus designed was a matrix of Helmholtz resonators which had its absorption peak below the 1T mode of the duct as this was where all of the testing was done.

E.) Data Reduction and comparison with theoretical predictions

The experimental data was both taken and reduced by hand. The data reduction was not a very time consuming process as all that had to be done was subtract the reference microphones values of the amplitude and phase from the values measured at the driver plane and the radiation measurements in the field. This was done so as to negate any shift in the measured amplitude or phase by the signal filters.

The computer programs were then run for the same conditions (i.e., driver power and frequency) as the experimental tests. These results were then compared with the experimental results and a brief error analysis was done.

F.) Determination of the "effective" liner admittance

The results of the experimental tests and the theory were found to be in very good agreement except near the calculated absorption peak of the liner. It was determined that the Garrison theory[5] used to calculate the theoretical liner admittances was probably at fault. Systematic computer runs were then performed parametrically varying the admittance until good agreement was obtained between the theoretical and experimental results.

Included in this report is a list of all the publications generated by this research effort. This is included as Appendix A. Also, Appendix B contains a list of all the conference presentations pertaining to the work performed under this contract and, finally, a copy of the most recent publication that was a direct result of the research performed in the past year on this contract is included as Appendix C.

A. Calibration of the Anechoic Chamber

The anechoic chamber is 10' by 13' by 6 1/2' in height. It has approximately 2' of sound absorbing fiberglass insulation in the floor, walls, and ceiling. A plan view of the anechoic chamber is presented in Fig. 8 of Appendix C.

It was necessary to calibrate the anechoic chamber with all of the microphone stands and the mounting stand for the test apparatus in place so that an estimate of the experimental errors in the free field measurements caused by this apparatus could be made. A University acoustic driver was mounted vertically on the support pedistal for the test apparatus, 37.5" off the floor, so that it would radiate sound equally in all directions, thus approximating a simple source. A ½" diameter Brüel and Kjaer microphone was placed 42.5" from the driver in the field and was used as a reference microphone for the amplitude readings.

A ¼" diameter B & K microphone was then moved in the direction that the test ducts would face, to be henceforth known as direction 1, (See Fig. 8, Appendix C and Fig. 1.) and measurements were taken every 5" out to 45". This procedure was repeated in the direction of the door of the chamber (90^{o} to the original direction of travel) and again measurements were taken every 5" up to 45" from the driver. This will be referred to as direction 2. At each microphone position measurements were made of the amplitude and phase, relative to the driver input signal, at frequencies from 300 to 750 Hz at 50 Hz increments as the tests were all to be run in this range. It should be noted here that the lower limit was imposed by the University driver and that the upper limit was imposed by the requirement that all of the tests be

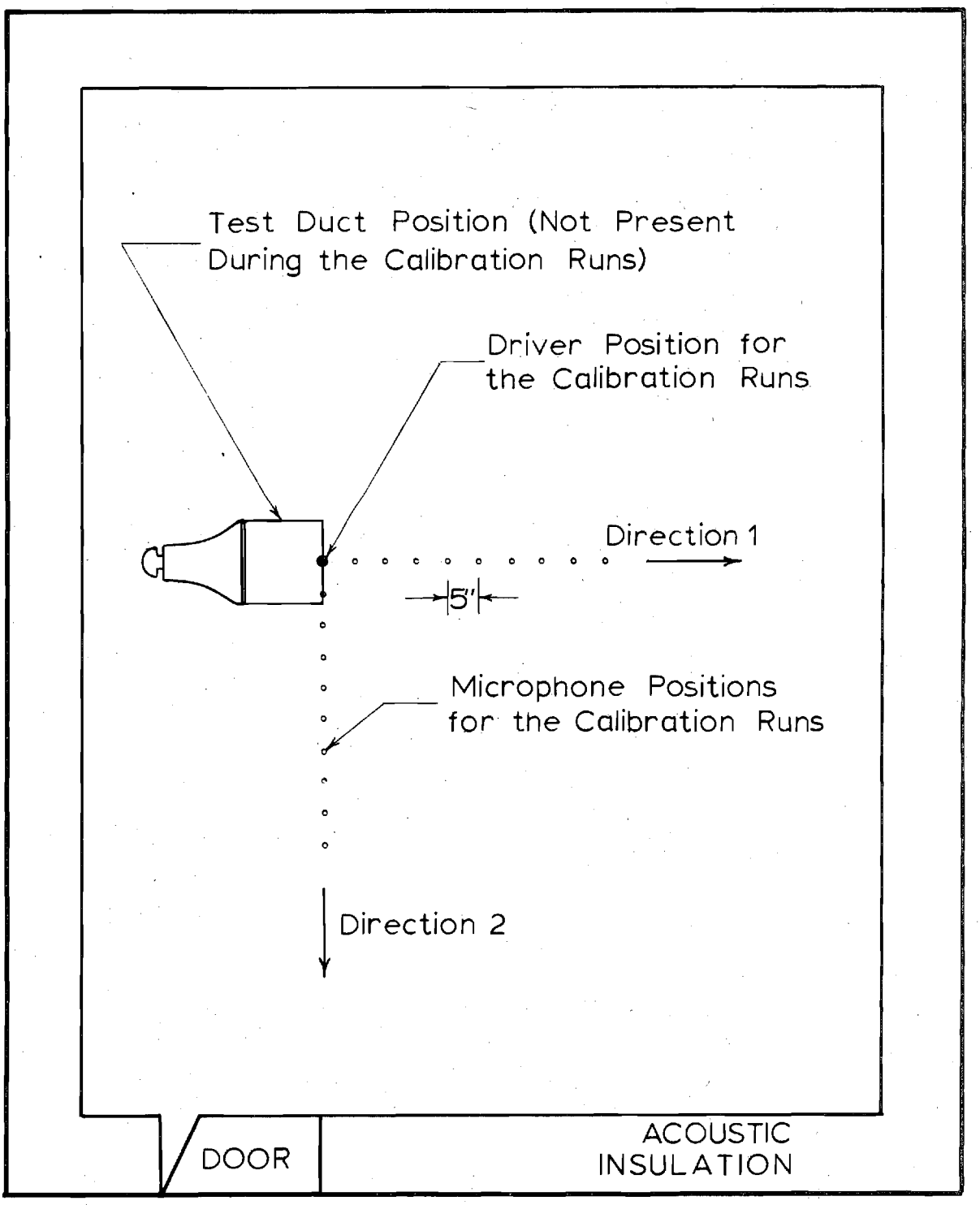

Fig. 1. Plan View of Anechoic Chamber with Driver and Microphone Positions for the Calibration Runs.

run below the 1T mode of the inlet and the straight duct. The latter requirement was to facilitate the data reduction and comparison with the theoretical model and the fact that we had no simple method of driving higher modes in the test ducts.

Results of the amplitude calibration in direction 1 are presented in Fig. 2. The solid lines are the theoretical curves for the Sound Pressure Level in decibels for a simple source in a free field. The equation for these curves is

$$SPL(dB) = -20 \log r \tag{1}$$

where r is the distance from the source. In this plot the amplitude is referenced to the 5" position. The worst point in this direction is at 30" and 350 Hz where the measured reading is 3.5 dB below the theoretical exact curve. All of the test runs were made with the microphones at 40" where the error was always less than 3 dB at all frequencies.

The results of the amplitude calibration in direction 2 are presented in Fig. 3. The worst point in this direction occurs at 30" and 400 Hz where the measured sound pressure level is 9.5 dB below the free field prediction. Again, all of the test runs were made with the microphones at 40" where the error was always less than 3 dB.

In Figs. 4 and 5 the phase comparisons are presented. The X's in these plots denote points where no stable phase reading could be obtained. This was later found to be caused by widely different signal strengths (i.e., voltages) being fed into the phase meter. This was corrected in subsequent tests by using another microphone signal as the reference input rather than

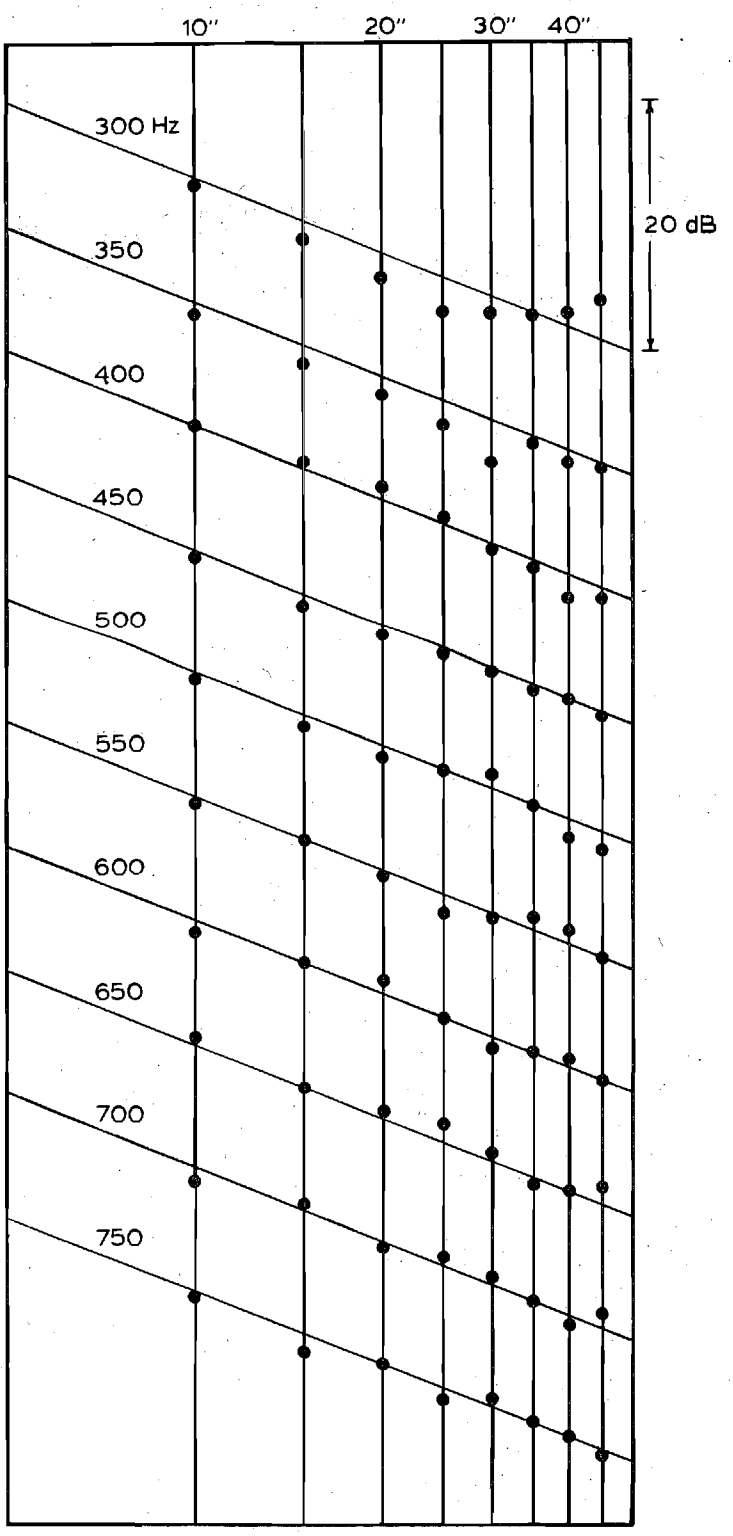

Fig. 2. Anechoic Chamber Acoustic Amplitude Calibration Direction 1.

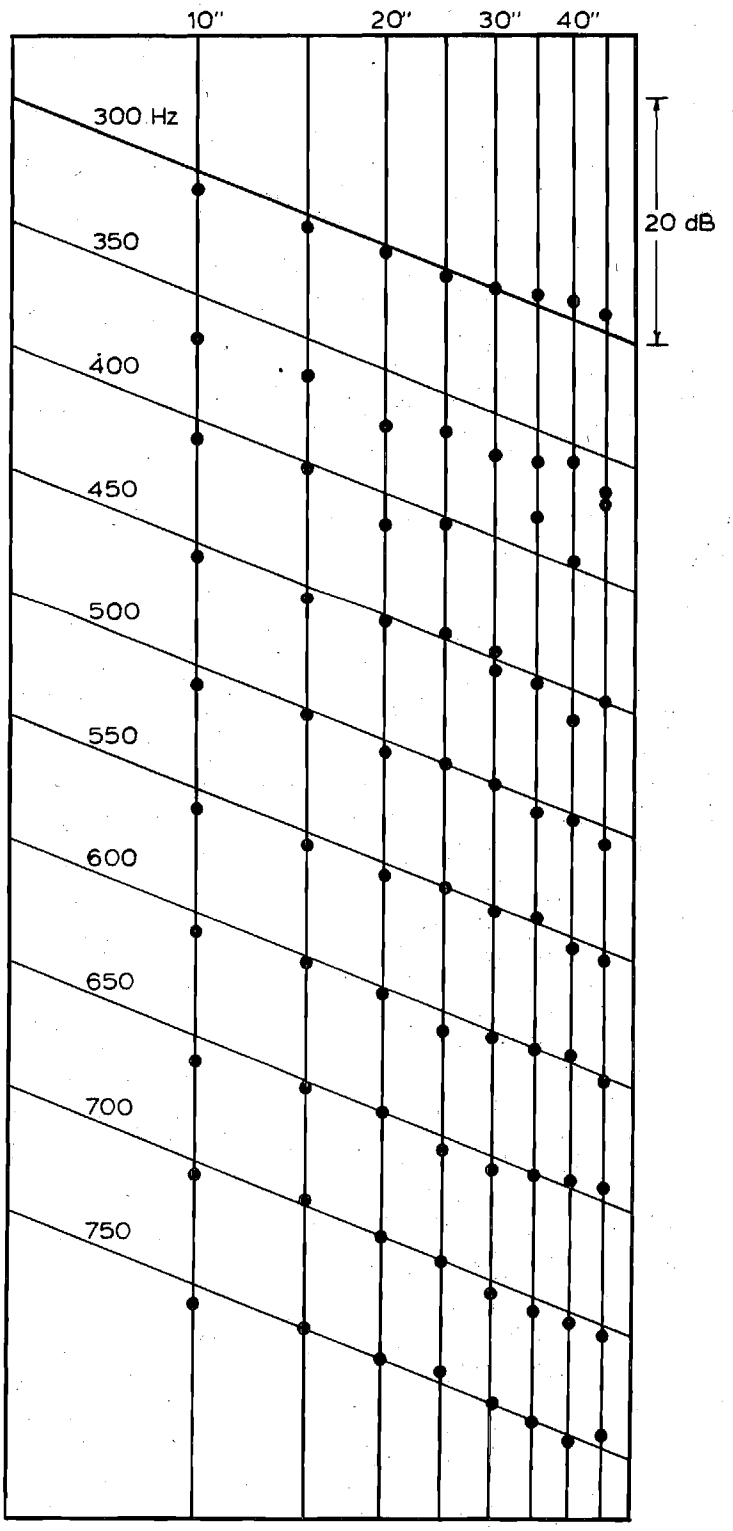

Fig. 3. Anechoic Chamber Acoustic Amplitude Calibration Direction 2.

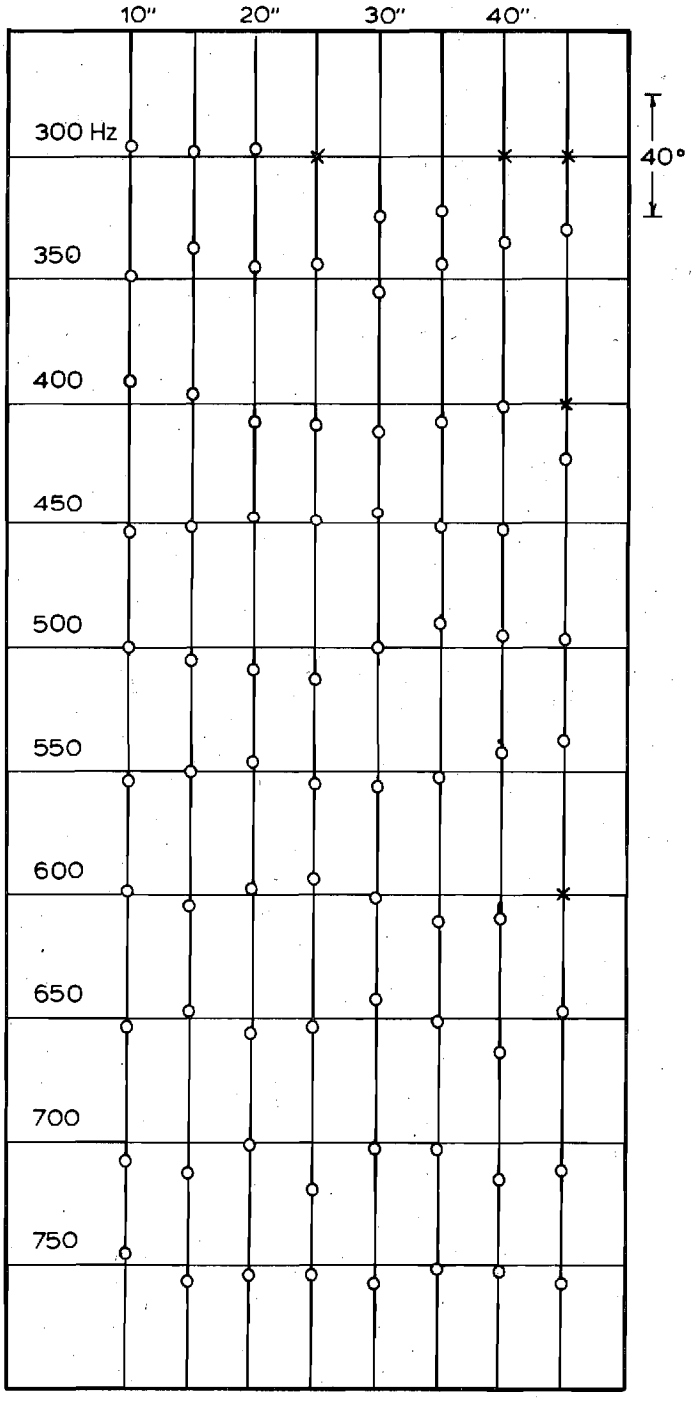

Fig. 4. Anechoic Chamber Acoustic Phase Calibration Direction 1.

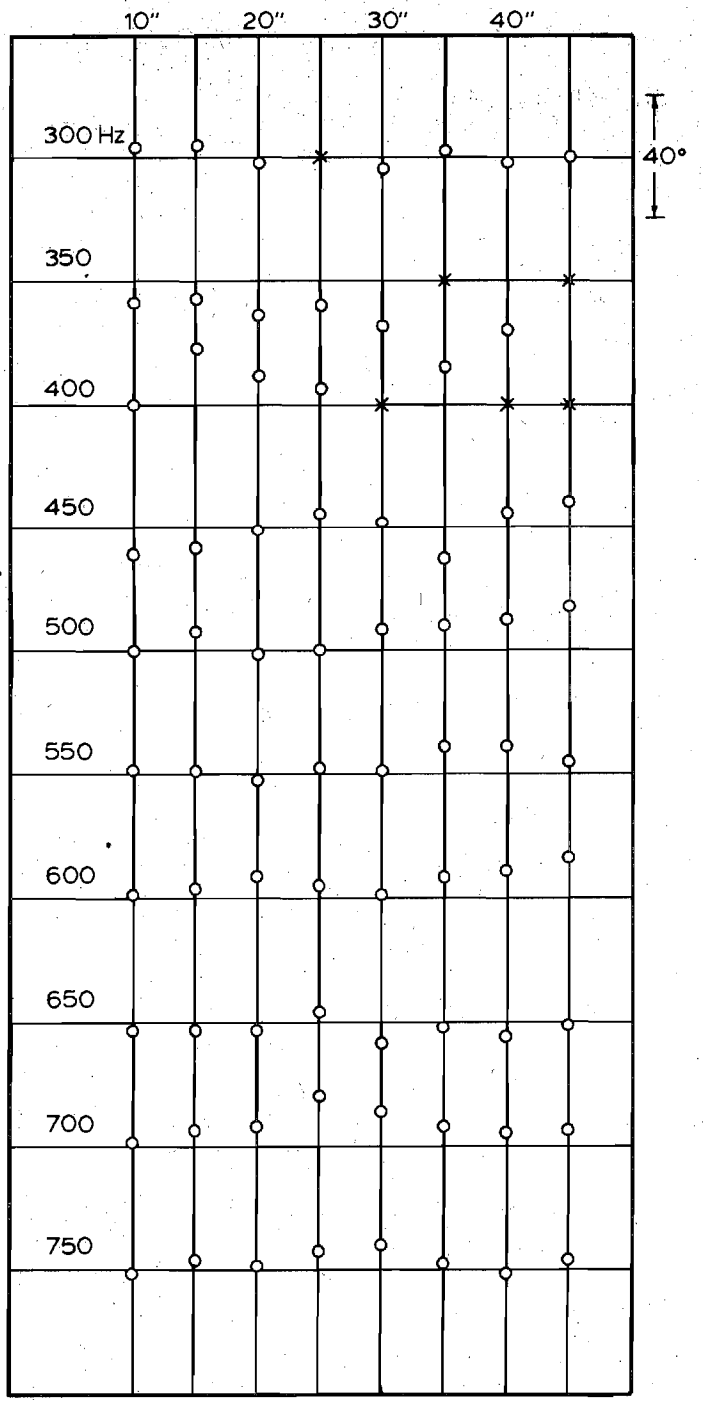

Fig. 5. Anechoic Chamber Acoustic Phase Calibration Direction 2.

the output from the oscillator that drove the acoustic driver. As can be seen most of the results are within 10^{o} of the values that were calculated using the simple source in a free field assumption. Some values are in error by as much as 20^{o} (See Fig. 4, direction 1 at 30" and 35" from the driver for 300 Hz.); however, these "bad" results are suspect as the phase meter could not be stabilized at adjacent points. The test results in these plots are referenced to the 5" position as it was closest to the driver and therefore subject to the least interference. This is a source of error that could potentially bias the results at a given frequency since if the phase reading at the 5" position was high the rest of the values at all other distances would be low by that amount and vice versa. It is conjectured that this is what happened at a couple of frequencies such as 600 and 700 Hz in Fig. 5.

From the calibration runs that were performed in the anechoic chamber with all of the support equipment for the model and the microphones in place it was concluded that the results obtained from tests in the chamber would be accurate to at least 3 dB in amplitude and 10^{o} in phase. As a matter of fact, the results obtained from tests in the chamber were in general found to be in better agreement with the theoretically calculated "exact" results than the calibration runs would lead one to expect.

B. Set-up of the Electronic Equipment

The equipment set-up can be basically broken down into two separate entities; the sound generating equipment and the sound measuring equipment. During the calibration of the anechoic chamber (See previous section.) these two systems were linked in that the oscillator that produced the driver signal was also used as a phase reference for the sound readings. This arrangement was changed in all subsequent tests as it was found that due to the large voltage difference in the signal strengths between a microphone and the oscillator the phase meter would not stabilize if the signals were close to 180^{o} out of phase. This being the case, another microphone was used as the reference in subsequent tests.

In all of the tests, a 75 watt University Sound heavy-duty driver was employed. The University driver was powered by a Krohn-Hite, Model DCA-50R, wide-band 50 watt amplifier which is capable of amplifying signals from D.C. to 500 KHz. A Model MT-56 Krohn-Hite matching transformer was used to match the impedances of the amplifier and the driver to get maximum power out of the driver. The amplifier was triggered by a Hewlett-Packard Model 202C low frequency oscillator which can produce signals from 1 Hz to 100,000 Hz. The frequency output of the oscillator was constantly monitored by two time base counters; one with fast response for ease of setting the desired frequency and one with slow response for checking the accuracy of the set frequency. The first was a Hewlett-Packard Model 5302 A 50 MHz universal counter and the second was a Monsanto Model 104 A preset/variable time-base counter. In all of the

conducted tests the frequency was always set to within $\pm$ 0.2 Hz of the desired frequency before any measurements were made.

For the actual sound measurements two sizes of Brüel & Kjaer microphones were used; ½ inch microphones were used outside the test duct for the field measurements and ¼ inch microphones were used inside the duct for reference and driver power measurements (See Figs. 4 and 7 of Appendix C.). Also, two different types of pre-amplifiers were used on these microphones; tube type which require a heating element voltage input and transistor type which do not.

The ¼ inch microphones were used with the tube type pre-amplifiers and the signals from these microphones were fed into a B & K two channel microphone selector, Type 4408, and from there into a B & K microphone amplifier, Type 2604. The ½ inch microphones were used with the transistor type pre-amplifiers. In each of the tests two ¼ inch microphones were used and five ½ inch microphones were used. To multiplex the five ½ inch microphone signals an in house fabricated five channel microphone selector was used and these were fed into a B & K Type 2606 measuring amplifier. Both of the B & K amplifiers gave direct decibel readings for the microphones to 0.1 dB, although the readings were certainly not reliable to this accuracy due to amplifier and pre-amplifier drift (this will be discussed in detail in the following section). The two microphone multiplexers were necessary as each of the measuring amplifiers could only handle one microphone at a time.

Although the signals were good enough to give reliable decibel readings they had to be pre-conditioned before good, steady phase

measurements could be made. To achieve this, two Krohn-Hite Model 3202 R filters were used. Both of the microphone signals, one being used as the reference signal, were passed through both a high and a low pass filter. These filters were set for all of the tests at 250 Hz for the high pass and 800 Hz for the low pass as all of the tests were run between 300 and 750 Hz. The phase was measured by a Wavetek Model 740 phase meter and was displayed in degrees (-180^{o} to 180^{o}) on a Fluke 8000 A digital multimeter.

Finally, all of the signals were run through an H-P 180 A dual beam oscilloscope. This was used to keep a check on the equipment by constantly checking the signal quality. Also, this was used to check if any of the equipment was being over driven or saturated at any given set of test conditions.

C. Conduct of the Experiments

As stated before, each of the tests was performed twice on separate days for verification of the data as it was read directly from meters and transcribed by hand. The results that are shown for the experimental tests are in fact an average of the two tests run for each experimental configuration. Also, the ambient temperature was monitored during each test so that corrections could be made for the varying speed of sound and the ambient pressure was measured before and after each run so that the characteristic impedance of the medium (i.e., the air in the anechoic chamber) could be calculated. The latter measurement was only important when a lined configuration was being tested.

Since nine measurements were made in the field for each test frequency and since only five ½ inch microphones and stands were available, four of the microphones had to be moved during each test. The fifth microphone, on the centerline of the test duct, was never moved and was used as a reference to check that the test conditions (i.e., the driver power output) were the same with the other microphones in both positions. A second reference microphone, a ¼ inch one, was placed in the nozzle section of the test set-up (See Figs. 4 and 7 of Appendix C.) just in front of the University driver so that a second independent check of the driver power output could be made for each test condition.

The sequence of events for each test was the same so, for the sake of simplicity, the straight duct will be used as the example here. The only difference lies in the fact that the straight duct was run with both hard and soft walls while the inlet configuration was only run with a hard wall.

First, the test duct was set-up in its soft walled configuration (i.e., with its liner exposed). The microphones were then set-up at 40 inches from the center of the entrance plane of the duct at 22.5^{o} increments from the centerline of the duct (See Fig. 8 Appendix C.). This was accomplished by triangulation and the ½ inch microphones were placed within at least one half inch of their ideal location. The microphones were then calibrated using a B & K pistonphone acoustic calibrator and the barometric pressure was noted. Then, the temperature in the chamber was read and the chamber was closed. Next, the oscillator was set to the desired frequency and the driver power was set by making the microphone at the imaginary driver plane read some pre-selected dB level. All of the other microphones phases and amplitudes were then read and recorded. The chamber was then opened and the temperature was rechecked. The chamber was closed and the test was repeated at a new frequency. The inlet was run at frequencies from 300 to 750 Hz at 50 Hz increments while the straight duct was tested over a frequency range up to 700 Hz. This was due to the different characteristic lengths of the two test bodies.

Once the desired frequency range had been tested, the liner in the duct was taped over so that it was no longer exposed, the microphones were recalibrated, and the whole test procedure was repeated. Having done this the four microphones in the field were moved to their intermediate positions, recalibrated, and another run was made of all the frequencies. Finally, the tape was removed from the liner, the microphones recalibrated again and the final set of measurements were made. Having done all this, the microphones were calibrated one last time and the barometric pressure

was re-read.

Each one of these tests took an entire day and required only one person most of the time. Two people were required when the microphones were calibrated, one in the chamber with the pistonphone and the other outside recording the dB levels.

D. Prediction of the Tested Liner Admittance*

For the lined walled tests, a liner was designed using the theory of Garrison.[5] The liner consisted of a matrix of 180 Helmholtz resonators (See Fig. 5 Appendix C.), 9 axial rows by 20 radial rows. It was designed so that its maximum effectiveness (i.e., resonance peak) occurred within the range of frequencies used in testing; that is, between 300 and 700 Hz, below the 1T mode of the duct and above the driving floor of the University driver. The tests were also all run in the liners linear regime as calculated by the theory.[5]

In the Garrison theory the linear regieme is defined as where the maximum acoustic velocity at the orifice of the Helmholtz resonator is below 60 ft./sec.. Using this criterion it is found that the linear regime is below the decibel levels in Table I for a sea level standard atmosphere and the respective driving frequencies. Since in all of the runs the decibel level was always less than 135 dB the linear liner theory was used.

Using the linear theory, the specific acoustic impedance of the liner is given by

$$Z = \theta - iX \tag{2}$$

where the specific acoustic resistance is given by

$$\theta = \frac{4}{\sigma \bar{\rho} c} (\pi \bar{\mu} \bar{\rho} f)^{\frac{1}{2}} (1 + t/d) \tag{3}$$

---

* See Nomenclature at the end of this section.

Table I

Maximum SPL(dB) where a Helmholtz resonator exhibits linear behavior

Frequency (Hz)	SPL (dB)
300	163
350	160
400	157
450	153
500	148
550	143
600	148
650	152
700	155

and the specific acoustic reactance by

$$X = \frac{2\pi f_o l_{eff}}{\bar{c}\,\sigma}\left(\frac{f}{f_o} - \frac{f_o}{f}\right) \tag{4}$$

In these equations the effective orifice length is given by

$$l_{eff} = t + 0.85\,d\left(1 - 0.7\sqrt{\bar{\sigma}}\right) \tag{5}$$

and the resonant frequency of a Helmholtz resonator by

$$f_o = \sqrt{\frac{\bar{\sigma}}{L l_{eff}}} \tag{6}$$

For the test conditions these are found to be given as

$$\theta = 0.01398\sqrt{f}$$

$$X = 10.186\left(\frac{f}{f_o} - \frac{f_o}{f}\right) \tag{7}$$

where the resonance peak of the liner f_o is found to be at 558 Hz. These values are related to the acoustic admittance of Appendix C defined as $y = V/\Phi$ by

$$y = -ik\left(\frac{1}{Z}\right) \tag{8}$$

where Z is defined with an inward facing normal and y is defined with an outward facing normal; thus the minus sign.

Using the definition of the absorption coefficient α; that is,

$$\alpha = \frac{4\theta}{(1+\theta)^2 + X^2} \tag{9}$$

it is found that the liner absorption curve is very "peaky" (See Fig. 6.). This being the case normal machining errors of 0.0005" were introduced into the admittance calculation and the resonance frequency was found to change by 1.5 Hz. It was found that this change in the resonance frequency could change the results at 550 Hz (i.e. the test frequency closest to the resonant frequency) by 3 dB and 5 degrees.

This will be discussed further in the ensuing sections as good agreement was obtained between the theory and experiment except at 550 Hz for the soft walled duct. It is felt that this disagreement is more the fault of the liner design approach at frequencies close to resonance rather than inaccuracies in the integral equation formulation.

Fig. 6. Absorption Coefficient vs. Frequency for Liner at Test Conditions.

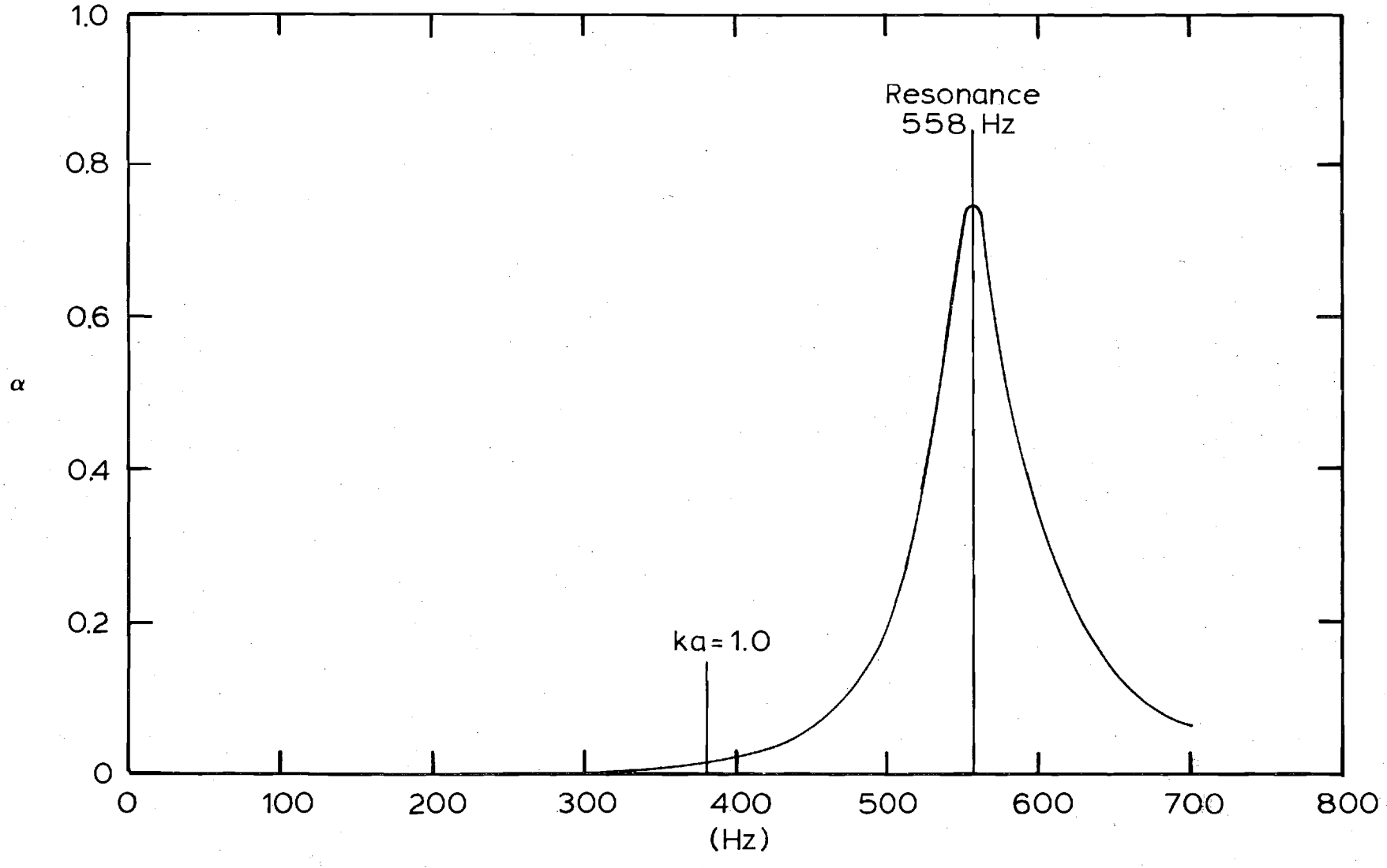

Nomenclature

a	characteristic length of the body
$\bar{c}$	speed of sound
d	Helmholtz resonator orifice diameter
f	frequency
f_o	resonant frequency of a Helmholtz resonator
i	$\sqrt{-1}$
k	wave number
L	backing depth of a Helmholtz resonator
l_{eff}	effective orifice length of a Helmholtz resonator
t	orifice length of a Helmholtz resonator
V	cylindrically symmetric normal acoustic velocity
y	acoustic admittance
Z	specific acoustic impedance of the liner
α	absorption coefficient of the liner
σ	open area ratio of the liner
$\bar{\sigma}$	open area ratio of a Helmholtz resonator
$\bar{\rho}$	density of the medium
$\bar{\mu}$	coefficient of viscosity of the medium
Φ	cylindrically symmetric acoustic potential
θ	specific acoustic resistance
X	specific acoustic reactance

E.) Data Reduction and Comparison with Theoretical Predictions

In the data reduction the speed of sound, the density, and the coefficient of viscosity were corrected for atmospheric conditions. The speed of sound determines the wave number from the frequency and is therefore extremely important in the data reduction for all cases while the density and coefficient of viscosity are only important in the theoretical admittance calculation (See Eq. (3).).

It should be pointed out that the theoretical and experimental models used in this study were not identical (See Figs. 3 and 4 for the straight duct configurations employed and Figs. 6 and 7 for the inlet configurations used in Appendix C.). The theoretical bodies were given hemispherical rear terminations in the interest of conserving computing time and space. It has been found, however, through theoretical studies using the integral equation formulation of the problem, that the exact form of the rear termination of a body has little effect on the sound field radiated to the forward half plane. Since the forward half plane is where all of the experimental measurements were made this is not considered to be a source of major errors.

In both experimental models the University driver was placed at the throat of a nozzle section (See Figs. 4 and 7 Appendix C.) so that the sound waves are plane at the driver plane. This was checked experimentally and the sound waves at the driver plane were found to be plane within 1 dB in amplitude and 5^{o} in phase. The amplitude was measured at this plane and was used as the input for the computer programs. The phase was not measured directly here as all of the other phase measurements were referenced to this microphone.

The straight duct was tested in both a hard walled configuration and in a lined configuration. For the hard walled tests the orifices of the Helmholtz resonators of the liner were simply covered with tape. The inlet tested had an L/a (length/radius) ratio of 2.0. The exact mathematical forms of the curves that make up the inlet contours can be found in Ref. (4). It should be noted here that in the experimental inlet model the centerbody was held in place by four small wing sectional struts set at 90^{o} from each other. Measurements of the driver amplitude were taken between two of these struts.

A comparison between the predicted and measured amplitudes for the hard walled inlet are presented in tabular form in Table II. It should be recalled that the presented experimental data is actually the average of results obtained in two completely separate tests. The average absolute errors between the experimental and theoretical results are included at each frequency. The results are presented on a quarter circle with a radius of 40" centered at the duct entrance plane (See Fig. 8 Appendix C.). The experimentally measured amplitude at the driver plane is also included. The phase results are presented in Table III. The driver phase is taken to be zero as it is the reference phase. The results for the inlet are plotted for 600 Hz in Fig. 11 of Appendix C.

As can be seen from Tables II and III the average absolute error between the theoretical and experimental results for the inlet configuration is always less than 3 dB in amplitude and 10^{o} in phase. At this juncture it seems appropriate to discuss some of the sources of error and their estimated magnitude so as to put the difference between the experimental

Table II.

Averaged Experimental/Theoretical Amplitudes for the Inlet 40" from Entrance Plane (SPL in dB)

Freq. (Hz) / Degrees Off ℄	300	350	400	450	500	550	600	650	700	750
0	96.6 93.8	96.6 96.2	98.9 99.1	104.2 103.1	108.1 108.4	113.6 113.1	110.3 110.8	107.9 108.1	109.0 106.6	109.5 106.0
11.25	95.9 93.8	96.1 96.1	99.5 99.1	103.5 103.0	108.6 108.3	113.0 112.9	110.0 110.7	108.4 107.9	107.9 106.4	108.5 105.8
22.5	95.3 93.6	96.3 95.9	99.1 98.8	102.4 102.7	109.1 108.0	111.0 112.5	110.6 110.2	107.5 107.5	107.3 105.9	107.2 105.3
33.75	94.7 93.3	97.0 95.6	98.1 98.5	103.5 102.3	107.8 107.4	110.7 111.9	110.2 109.5	107.4 106.7	106.3 105.1	105.6 104.4
45	93.9 93.0	96.9 95.2	97.9 98.0	103.4 101.7	105.8 106.7	111.4 111.1	108.5 108.6	105.9 105.7	104.6 104.1	105.2 103.3
56.25	92.7 92.5	95.8 94.7	97.8 97.5	101.0 101.1	104.7 106.0	110.1 110.1	107.0 107.5	103.8 104.5	104.3 102.8	102.6 101.9
67.5	91.1 92.0	95.0 94.2	98.7 96.9	100.1 100.4	105.0 105.2	109.0 109.1	105.1 106.3	103.0 103.1	101.4 101.3	101.2 100.4
78.75	91.6 91.3	93.7 93.5	97.2 96.2	101.1 99.7	104.4 104.5	107.0 108.3	105.4 105.2	102.0 101.9	100.3 99.8	101.9 98.8
90	91.0 90.7	92.3 92.8	95.9 95.5	101.5 99.0	104.1 103.8	107.2 107.6	103.5 104.5	100.7 100.9	99.4 98.7	99.9 97.4
Driver	127.0	127.0	127.0	127.0	127.0	127.0	127.0	127.0	127.0	127.0
Average Absolute Error	1.18	0.72	0.54	1.01	0.54	0.60	0.59	0.30	1.09	2.03

Table III

Averaged Experimental/Theoretical Phases for the Inlet 40" from the Entrance Plane (Degrees Relative to the Driver)

Freq. (Hz) / Degrees Off ℄	300	350	400	450	500	550	600	650	700	750
0	-61 -66	-12 -13	35 41	98 98	170 167	-104 -92	7 8	72 79	130 141	-158 -160
11.25	-61 -66	-20 -13	41 41	80 99	165 167	-102 -92	5 8	72 79	134 141	-163 -160
22.5	-62 -66	-15 -13	46 41	80 99	170 168	-87 -92	3 8	75 79	137 140	-162 -160
33.75	-68 -65	-14 -12	41 42	76 100	174 168	-91 -91	-1 8	77 78	139 140	-166 -161
45	-68 -65	-12 -12	39 43	93 101	177 170	-93 -90	8 8	74 78	138 140	-167 -161
56.25	-65 -63	-16 -10	44 45	107 103	169 172	-91 -88	16 10	73 79	139 140	-153 -161
67.5	-63 -61	-23 -8	48 47	109 106	179 175	-93 -85	14 13	83 82	146 142	-162 -160
78.75	-61 -59	-20 -6	48 49	103 109	-173 179	-78 -80	11 18	93 87	143 147	-154 -156
90	-56 -54	-10 -2	43 53	107 113	-169 -177	-64 -75	27 25	94 94	147 154	-148 -149
Driver	0	0	0	0	0	0	0	0	0	0
Average Absolute Error	3.1	6.1	3.2	9.9	4.3	6.0	3.8	4.0	4.4	3.4

and theoretical results in prospective. First, there are the obvious experimental errors caused by microphone amplifier drift, temperature changes in the anechoic chamber of and the microphone placement in the chamber. Comparing test results and calibrations these errors are estimated to account for up to 0.5 dB in amplitude and 5 degrees in phase. Another source of error is the anechoic chamber which, as stated before, can account for errors up to 3 dB and 10 degrees. A more subtle source of experimental error is due to scale switching on the microphone amplifiers which can account for as much as 0.5 dB (i.e. 100 dB on the 90 to 110 dB scale reads as 100.5 dB on the 100 to 120 dB scale).

The theoretical errors are estimated by comparison with exact solutions for similar geometries. It is found that the computer programs introduce about 1% error, insignificant in dB but accounting for as much as 5 degrees in phase. Another source of error is the assumption of a plane wave at the driver plane; unfortunately the effect of this assumption can not be easily estimated. As none of the above mentioned errors are specifically geometry dependent, these error estimates apply to the straight duct configurations too.

The results of the experimental tests and of the computer runs for the hard walled straight duct configurations are presented in Tables IV and V. The amplitude results are tabulated in decibels in Table IV while the phase results in degrees appear in Table V. Again, the experimental results presented are actually the average of two separate runs.

It can be seen that all of the amplitude results are very good as the experimental and theoretical values at each test frequency have average

Table IV

Averaged Experimental/Theoretical Amplitudes for the Hard Walled Straight Duct 40" from the Entrance Plane (SPL in dB)

Freq. (Hz) / Degrees Off ℄	300	350	400	450	500	550	600	650	700
0	102.3 99.8	104.6 104.2	110.8 110.5	114.1 113.9	110.1 110.4	108.4 108.2	105.8 107.3	108.2 107.3	108.6 108.1
11.25	101.6 99.7	104.9 104.1	111.4 110.4	112.9 113.8	110.9 110.3	107.0 108.0	106.4 107.1	108.3 107.1	107.7 107.8
22.5	100.5 99.5	104.8 103.8	110.3 110.0	113.1 113.4	110.4 109.8	105.9 107.5	107.0 106.5	106.8 106.5	106.1 107.1
33.75	100.2 99.2	105.3 103.4	110.0 109.5	113.1 112.7	108.1 109.1	106.8 106.7	106.2 105.7	105.1 105.5	105.3 106.0
45	99.1 98.8	104.4 102.9	109.7 108.8	112.7 111.8	106.2 108.1	107.2 105.6	104.0 104.5	104.0 104.2	105.3 104.5
56.25	97.9 98.3	103.5 102.3	108.7 108.0	109.5 110.8	106.3 106.9	104.3 104.3	101.9 103.1	103.6 102.7	102.1 102.9
67.5	96.9 97.7	102.3 101.6	108.3 107.2	109.1 109.8	105.1 105.6	102.0 102.8	102.6 101.5	101.4 101.0	99.3 101.1
78.75	96.7 97.0	101.5 100.9	107.0 106.4	110.2 108.9	103.9 104.4	100.3 101.4	101.5 99.8	99.9 99.3	100.5 99.3
90	96.7 96.3	99.7 100.2	105.2 105.8	108.4 108.1	103.9 103.5	100.7 100.2	98.9 98.4	98.8 97.6	95.5 97.6
Driver	126.9	126.9	126.9	126.9	126.9	126.9	126.9	126.9	126.9
Average Absolute Error	0.96	0.96	0.67	0.70	0.71	0.77	0.91	0.68	1.00

Table V

Averaged Experimental/Theoretical Phases for the Hard Walled Straight Duct 40" from the Entrance Plane (Degrees Relative to the Driver)

Freq. (Hz) / Degrees Off ℄	300	350	400	450	500	550	600	650	700
0	-62 -65	-8 -8	69 65	-177 180	-82 -90	-17 -24	37 37	96 96	164 156
11.25	-63 -65	-12 -8	74 65	179 180	-82 -90	-5 -24	34 37	99 96	169 156
22.5	-67 -65	-9 -7	72 66	172 180	-78 -90	-7 -24	33 36	107 95	163 155
33.75	-73 -64	-7 -6	68 66	-175 -180	-81 -90	-10 -24	39 36	106 95	156 154
45	-72 -63	-10 -5	68 68	-174 -179	-89 -90	-16 -25	46 35	93 94	161 154
56.25	-64 -61	-13 -3	78 70	-167 -176	-87 -88	-4 -24	39 36	102 94	170 153
67.5	-61 -59	-15 0	80 74	179 -173	-77 -85	-11 -21	32 37	116 95	158 154
78.75	-58 -56	-7 3	75 78	-169 -167	-68 -79	-4 -16	33 42	107 99	167 157
90	-53 -52	9 8	67 83	-161 -161	-78 -72	10 -8	52 50	114 106	164 164
Driver	0	0	0	0	0	0	0	0	0
Average Absolute Error	3.7	5.3	6.0	4.6	7.1	14.0	4.3	8.0	7.7

absolute errors of one decibel or less. The phase results also compare very well except at 550 Hz where the average absolute error is about twice that at the other frequencies. The probable reason for this is that this frequency is very close to the tuning frequency of the liner, which is about 558 Hz (See Fig. 6.), and that the liner orifices were closed off with tape for the hard walled tests which may not have been 100 percent effective in keeping the liner from influencing the phase results. It should be noted, however, that this method of closing off the liner was effective as far as the amplitude results are concerned (See Table IV.). The amplitude and phase results at 550 Hz are plotted in Fig. 9 of Appendix C for this case.

The experimental and test results for the case of the soft, lined walled straight duct configuration are tabulated in Tables VI and VII for the amplitude and phase, respectively. The results for the amplitude and phase at 500 Hz are plotted in Fig. 10 of Appendix C. The errors in the amplitude are in general less than 3 dB and the errors in the phase less than 10 degrees except at 550 Hz where the errors for both the amplitude and the phase are very large. These differences between the theoretical and experimental results are probably due to the liner theory used for calculating the admittance of the liner and machining errors in the manufacture of the liner.

Table VI

Averaged Experimental/Theoretical Amplitudes for the Soft Walled Straight Duct 40" from the Entrance Plane (SPL in dB)

Freq. (Hz) / Degrees Off ℄	300	350	400	450	500	550	600	650	700
0	103.8 101.7	110.1 108.3	112.9 113.9	108.0 107.6	104.7 104.9	88.2 70.9	101.2 104.2	109.1 108.9	108.1 108.0
11.25	103.0 101.6	110.3 108.2	113.6 113.7	106.9 107.5	105.6 104.7	87.0 70.4	102.0 104.0	109.3 108.7	107.1 107.7
22.5	102.9 101.4	110.4 107.9	112.5 113.4	106.5 107.0	104.9 104.2	85.8 69.1	102.4 103.5	107.8 108.1	105.3 107.0
33.75	102.3 101.1	110.6 107.5	112.1 112.8	107.2 106.4	102.5 103.5	86.3 67.1	101.8 102.6	106.4 107.1	104.7 105.9
45	101.4 100.6	109.9 107.0	111.7 112.1	105.8 105.5	101.6 102.5	86.5 65.4	99.6 101.5	105.1 105.9	104.7 104.5
56.25	99.4 100.1	108.8 106.3	110.9 111.3	103.5 104.5	101.1 101.2	83.9 65.8	97.7 100.2	104.7 104.4	101.5 102.9
67.5	98.8 99.6	107.6 105.7	109.5 110.5	102.6 103.4	100.1 100.0	80.1 67.2	98.2 98.7	102.5 102.7	99.3 101.1
78.75	99.0 98.9	106.0 105.0	109.0 109.8	103.3 102.5	99.8 99.8	76.6 68.1	96.6 97.1	101.0 101.0	99.8 99.3
90	99.1 98.2	104.1 104.3	107.4 109.1	101.3 101.8	99.6 97.9	79.2 68.0	93.6 95.6	99.9 99.3	94.5 97.5
Driver	126.9	126.9	126.9	126.9	126.9	126.9	126.9	126.9	126.9
Average Absolute Error	1.06	2.00	0.78	0.63	0.62	15.73	1.59	0.41	1.17

Table VII

Averaged Experimental/Theoretical Phases for the Soft Walled Straight Duct 40" from the Entrance Plane (Degrees Relative to the Driver)

Freq. (Hz) / Degrees Off ℄	300	350	400	450	500	550	600	650	700
0	-61 -63	9 4	143 134	-125 -129	-49 -59	11 79	-57 -65	65 69	151 144
11.25	-63 -63	6 4	147 134	-130 -129	-48 -59	15 80	-65 -65	68 69	155 143
22.5	-67 -62	9 4	146 134	-131 -129	-45 -59	16 82	-66 -65	76 68	148 143
33.75	-71 -61	12 5	142 135	-125 -128	-47 -59	9 89	-57 -66	75 68	143 142
45	-69 -60	7 7	143 137	-118 -127	-55 -59	7 106	-45 -66	62 67	147 141
56.25	-64 -59	3 9	152 139	-116 -125	-52 -58	10 123	-57 -65	72 67	156 141
67.5	-61 -56	2 11	155 142	-123 -122	-43 -54	6 129	-68 -64	85 69	143 142
78.75	-57 -53	12 15	148 147	-120 -116	-36 -49	19 126	-48 -60	69 72	156 145
90	-50 -50	25 19	142 152	-109 -110	-47 -41	43 120	-42 -52	86 80	152 152
Driver	0	0	0	0	0	0	0	0	0
Average Absolute Error	4.4	4.8	9.3	3.8	9.7	88.7	8.1	6.1	6.4

F. Determination of the "Effective" Liner Admittance

As stated in the previous sections normal machining errors can change the resonant frequency of the liner by as much as 1.5 Hz which can change the sound field by as much as 3 dB and 5 degrees due to the liners "peaky" absorption curve (See Fig. 6.). Even this can't, however, account for the large differences between the experimental and theoretical results at 550 Hz for the lined straight duct. Noteing that the calculated results were consistently lower than those measured, it was assumed that the liner theory[5] predicted the admittance (i.e. the effectiveness) of the liner to be higher than it actually was. To check this hypothesis a parametric set of computer runs was conducted in which the admittance was systematically varied to see if the true "effective" admittance of the liner at 550 Hz could be determined by comparison with the experimental results. From this set of computer runs it was found that the true "effective" admittance of the liner was approximately

$$y = -0.13 - i0.28 \qquad @\ 550\ \text{Hz} \tag{10}$$

which is the real part of the admittance calculated from Eqs. (2-4) and (8) multiplied by 0.35 and the imaginary part multiplied by 0.65. The experimental and theoretical results, calculated using the admittance in Eq. (10), are tabulated in Table VIII. As can be seen these results are more in line with what was found at the other frequencies (See Tables VI and VII.), so it is concluded that the Garrison theory of Ref. (5) does not give the proper admittance for this type of liner near resonance (i.e. it predicts the

Table VIII

Averaged Experimental/Theoretical Acoustic Radiation 40" from the Entrance Plane of the Soft Walled Straight Duct at 550 Hz with $y = -0.13 - i\,0.28$

Degrees Off ℄	Amplitude SPL (dB)	Phase (degrees)
0	88.2 89.7	11 15
11.25	87.0 89.5	15 14
22.5	85.8 88.9	16 13
33.75	86.3 88.0	9 12
45	86.5 86.8	7 12
56.25	83.9 85.3	10 13
67.5	80.1 83.7	6 17
78.75	76.6 82.4	19 24
90	79.2 81.7	43 34
Average Absolute Error	2.49	4.9

admittance to be too high). This exercise also points out that the integral equation technique can be used to determine a liners true "effective" admittance from experimental measurements in the field.

References

1.) Meyer, W. L. , Bell, W. A., and Zinn, B. T., "Prediction of the Sound Field Radiated from Axisymmetric Surfaces," AIAA Paper No. 78-195, presented at the AIAA 16th Aerospace Sciences Meeting, Huntsville, Alabama, January 16-18, 1978.

2.) Meyer, W. L., Bell, W. A., Stallybrass, M. P., and Zinn, B. T., "Prediction of the Sound Field Radiated from Axisymmetric Surfaces," Journal of the Acoustical Society of America, Vol. 63, No. 2, pp. 631-638, March 1979.

3.) Meyer, W. L., Bell, W. A., and Zinn, B. T., "Sound Radiation from Finite Length Axisymmetric Ducts and Engine Inlets," AIAA Paper No. 79-0675, presented at the AIAA 5th Aeroacoustics Conference, Seattle, Washington, March 12-14, 1979.

4.) Miller, B. A., Dastoli, B. J., and Wesoky, H. L., "Effect of Entry-Lip Design on Aerodynamics and Acoustics of High-Throat-Mach-Number Inlets for the Quiet, Clean, Short-Haul Experimental Engine," NASA TM X-3222, Lewis Research Center, Cleveland, Ohio, May 1975.

5.) Garrison, G. D., "A Study ofthe Suppression of Combustion Oscillations with Mechanical Damping Devices," Phase II Summary Report, Pratt & Whitney Aircraft Co., PWA FR-1922, July 15, 1966.

Appendix A

Publications Generated by this Research Effort

A.) "Integral Solution of Three Dimensional Acoustic Radiation Problems," W. L. Meyer, W. A. Bell and B. T. Zinn, Proceedings of the International Symposium on Innovative Numerical Analysis in Applied Engineering Science, Versailles, France, May 23-27, 1977.

B.) "Predicting the Acoustics of Arbitrarily Shaped Bodies Using an Integral Approach," W. A. Bell, W. L. Meyer and B. T. Zinn, AIAA Journal, Vol. 15, No. 6, pp. 813-820, June 1977.

C.) "Prediction of the Sound Field Radiated from Axisymmetric Surfaces," W. L. Meyer, W. A. Bell and B. T. Zinn, AIAA Paper No. 78-195, presented at the AIAA 16th Aerospace Sciences Meeting, Huntsville, Alabama, January 16-18, 1978.

D.) "Boundary Integral Solutions of Three Dimensional Acoustic Radiation Problems," W. L. Meyer, W. A. Bell, M. P. Stallybrass and B. T. Zinn, Journal of Sound and Vibration, Vol. 59, No. 2, pp. 245-262, July 1978.

E.) "Prediction of the Sound Field Radiated from Axisymmetric Surfaces," W. L. Meyer, W. A. Bell, M. P. Stallybrass and B. T. Zinn, Journal of the Acoustical Society of America, Vol. 63, No. 2, pp. 631-638, March 1979.

F.) "Sound Radiation from Finite Length Axisymmetric Ducts and Engine Inlets," W. L. Meyer, W. A. Bell and B. T. Zinn, AIAA Paper No. 79-0675, presented at the AIAA 5th Aeroacoustics Conference, Seattle, Washington, March 12-14, 1979.

G.) "Acoustic Radiation from Axisymmetric Ducts: A Comparison of Theory and Experiment," W. L. Meyer, B. R. Daniel and B. T. Zinn, AIAA Paper No. 80-0097, presented at the AIAA 18th Aerospace Sciences Meeting, Pasadena, California, January 14-16, 1980.

Appendix B

Presentations Generated by this Research Effort

A. "Integral Solutions of Three Dimensional Acoustic Radiation Problems," Presented at the International Symposium on Innovative Numerical Analysis in Applied Engineering Science at Versailles, France, May 23-27, 1977. (Zinn)

B. "Prediction of the Sound Field Radiated from Axisymmetric Surfaces," Presented at the AIAA 16th Aerospace Sciences Meeting at Huntsville, Alabama, January 16-18, 1978. (Bell)

C. "Sound Radiation from Finite Length Axisymmetric Ducts and Engine Inlets," Presented at the 5th AIAA Aeroacoustics Conference at Seattle, Washington, March 12-14, 1979. (Zinn)

D. "Acoustic Radiation from Axisymmetric Ducts: A Comparison of Theory and Experiment," Presented at the AIAA 18th Aerospace Sciences Meeting, Pasadena, California, January 14-16, 1980. (Meyer)

Appendix C

AIAA Paper Number 80-0097 Presented at the AIAA 18th Aerospace Sciences Meeting, Pasadena, Calif., Jan. 14-16, 1980.

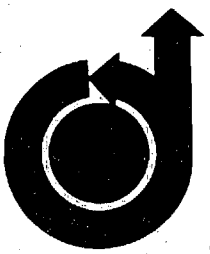

AIAA-80-0097

Acoustic Radiation from Axisymmetric Ducts: A Comparison of Theory and Experiment

W. L. Meyer, B. R. Daniel and B. T. Zinn, Georgia Institute of Technology, Atlanta, Ga.

AIAA 18th AEROSPACE SCIENCES MEETING

January 14-16, 1980/Pasadena, California

ACOUSTIC RADIATION FROM AXISYMMETRIC DUCTS: A COMPARISON OF THEORY AND EXPERIMENT†

W. L. Meyer*, B. R. Daniel‡ and B. T. Zinn**
School of Aerospace Engineering
Georgia Institute of Technology
Atlanta, Ga. 30332

Abstract

A special integral representation of the exterior solutions of the Helmholtz equation is used to calculate the free field acoustic radiation patterns around two finite axisymmetric bodies; a straight pipe and a jet engine inlet. The radiation patterns around these bodies are then measured experimentally, with the free field being approximated through the use of an anechoic chamber. The inlet tested has a hard wall while the straight pipe is tested with both a hard and a lined wall. The computed theoretical and the measured experimental acoustic radiation patterns are found to be in good agreement. A discussion of possible sources of error, both theoretical and experimental, is included.

Introduction

One of the major problems facing the aircraft industry today is to reduce the noise radiated to the ground from aircraft engines without sacrificing any of the overall efficiency of the aircraft. A major source of engine noise is the compressor or the fan noise which is radiated out of the jet engine through its inlet section. Research efforts directed toward reducing these noise sources have included, among other things, the reduction of the sound level in the jet engine inlet section, by adding sound absorbing materials (i.e., acoustic liners) to the inside of the engine inlet. Weight and volume of these acoustic liners are of prime concern to the aircraft industry as these are directly related to the overall efficiency of the aircraft; thus, efficient acoustic liner designs are sought. In the past, optimum liner designs have been found by extensive full scale testing of engines with various liner configurations which is a very costly and time consuming process. Most of this testing could be eliminated by the development and use of efficient, accurate analytical procedures for the prediction of the sound field radiated from lined jet engine inlets. The development of such a method, based upon a special integral representation of the radiation solutions of the Helmholtz equation, has been discussed at length by the authors of this paper in earlier publications[1-6]. In the present study the applicability of this integral solution technique is investigated by comparing its predictions with the results obtained from an experimental study.

Background

In this paper a special axisymmetric integral representation of the exterior solutions of the Helmholtz equation[3,4] is employed to theoretically calculate the free field acoustic radiation patterns surrounding two finite axisymmetric bodies; namely, a straight duct and a jet engine inlet configuration. The inlet used in these studies is the so called QCSEE inlet (i.e., the quiet, clean, short-haul experimental engine inlet of Reference 5). In previous studies by this group the sound fields radiated from complicated geometries with complex (mixed) boundary conditions were calculated using a solution procedure based on the aforementioned integral representation. The solutions generated were found to be in excellent agreement with "exact" solutions calculated by employing the method of Separation of Variables. A detailed development of the integral equations and solution procedures used along with many comparisons with exact solutions for various bodies, both 3-D and axisymmetric, can be found in Refs. (1-4 and 6). In this connection it should be pointed out that this theoretical technique and solution procedure have been found to be both accurate and computationally efficient when compared to other methods.

Theoretical Method

In this study a so called "integral technique" is employed to calculate the sound radiated from various axisymmetric configurations. The particular method is unique in that it is applicable at all nondimensional wave numbers ka (where k is the wave number and a is an appropriate body dimension), it contains no tangential derivatives on the surface of the body S (See Fig. 1.) and it contains no singular kernels which cannot be handled numerically by straight forward means.

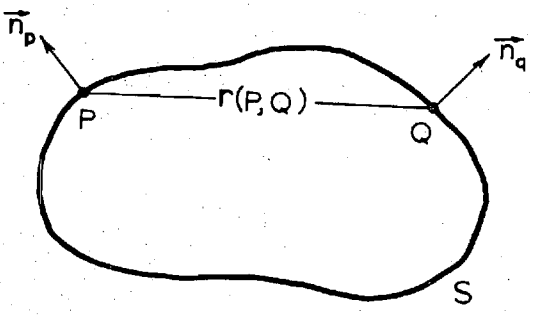

Figure 1. Definition of Elements on the Body.

The details of the derivation of the particular integral equations used are presented in Refs. (1, 2 and 6) and therefore will not be repeated here. The basic integral equation employed on the surface of the body is written in terms of the acoustic potential φ and it contains surface integrals over the surface of the body S. If we now define $\frac{\partial}{\partial n}$ as the outward normal derivative from the surface, P and Q as points on the surface with their unit outward normals defined as $\vec{n}_p$ and $\vec{n}_q$ respectively, and $\frac{\partial \varphi}{\partial n}$ as the normal acoustic velocity this integral equation takes the following general form

† This research was supported under AFOSR Contract # F49620-77-C-0066; Lt. Col. Lowell Ormand, Grant Monitor.
* Research Engineer, Member AIAA.
‡ Senior Research Engineer.
** Regents' Professor, Associate Fellow AIAA.

$$\iint_S \left\{ \phi(Q) \frac{\partial G(P,Q)}{\partial n_\xi} - G(P,Q) \frac{\partial \phi(Q)}{\partial n_\xi} \right\} dS_\xi + \frac{i}{k} \iint_S \left\{ [\phi(Q) - \phi(P)] \frac{\partial^2 G(P,Q)}{\partial n_P \partial n_\xi} - \frac{\partial G(P,Q)}{\partial n_P} \frac{\partial \phi(Q)}{\partial n_\xi} \right\} dS_\xi \qquad (1)$$

$$-\left(\frac{i}{k}\right) \phi(P) \iint_S (\vec{n}_P \cdot \vec{n}_\xi)(ik)^2 G(P,Q) dS_\xi = 2\pi \left(\phi(P) + \frac{i}{k} \frac{\partial \phi(P)}{\partial n_P} \right)$$

In this equation G(P,Q) can be any fundamental solution of the Helmholtz equation. In this study it has been chosen to be the free space Green's Function of the Helmholtz equation; that is

$$G(P,Q) = \frac{e^{-ikr(P,Q)}}{r(P,Q)} \qquad (2)$$

where r(P,Q) is the distance between the points P and Q on the surface of the body.

Once the acoustic potential is calculated on the surface of the body using Eqn. (1), the following integral representation for ϕ may be used to calculate the acoustic potential anywhere in the field surrounding the body. In this case the point P is no longer on the body S but in the field surrounding it.

$$\iint_S \left\{ \phi(Q) \frac{\partial G(P,Q)}{\partial n_\xi} - G(P,Q) \frac{\partial \phi(Q)}{\partial n_\xi} \right\} dS_\xi = 4\pi \phi(P) \qquad (3)$$

If the body of interest is axisymmetric, as most jet engine inlets are, certain simplifications may be made[3,4]. Let us now define a new cylindrically symmetric acoustic potential and normal acoustic velocity as

$$\Phi = \frac{\phi}{\cos m\theta}$$

$$V = \frac{\partial \phi}{\partial n} \Big/ \cos m\theta \qquad (4)$$

where m is the tangential mode number and θ is defined as in Figure 2

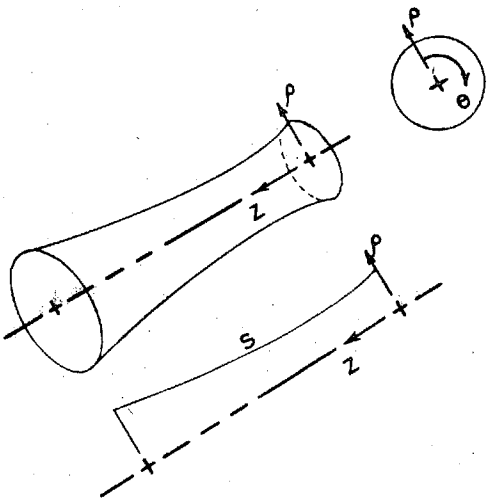

Figure 2. General Axisymmetric Geometry and 2-D Projection.

and s is the distance along the body in the ρ-z plane (e.g. $0 \le s \le \ell$). In doing this we have effectively separated out all the tangential modes; thus, the formulation that will be presented for axisymmetric bodies will be cylindrically symmetric in that all the tangential modes (i.e., m = 0,1,2...) may be solved for separately. Having these definitions, Eqn. (1) can be rewritten as

$$\int_0^\ell \Phi(Q) \left\{ K_1(P,Q) + K_2(P,Q) \right\} ds_\xi - \Phi(P) \int_0^\ell \left\{ F_1(P,Q) + F_2(P,Q) \right\} ds_\xi - \int_0^\ell V(Q) \left\{ I_1(P,Q) + I_2(P,Q) \right\} ds_\xi = 2\pi \left\{ \Phi(P) + \frac{i}{k} V(P) \right\} \qquad (5)$$

where s is the distance along the 2-D projection of the body in the ρ-z plane (See Fig. 2.). The kernel functions K_1 and K_2 are defined as

$$K_1(P,Q) = 2 \int_0^\pi \frac{\partial G(P,Q)}{\partial n_\xi} (\cos m\theta_\xi) \, d\theta_\xi$$

$$K_2(P,Q) = 2 \frac{i}{k} \int_0^\pi \frac{\partial^2 G(P,Q)}{\partial n_P \partial n_\xi} (\cos m\theta_\xi) d\theta_\xi \qquad (6)$$

The forcing functions are given by

$$F_1(P,Q) = 2\frac{A}{k}\int_0^{\pi} G(P,Q)(ik)^2(\vec{n}_P \cdot \vec{n}_\ell)\, d\theta_\ell$$

$$F_2(P,Q) = 2\frac{A}{k}\int_0^{\pi} \frac{\partial^2 G(P,Q)}{\partial n_P \partial n_\ell}\, d\theta_\ell \qquad (7)$$

and the influence functions are defined as

$$I_1(P,Q) = 2\int_0^{\pi} G(P,Q)(\cos m\theta_\ell)\, d\theta_\ell$$

$$I_2(P,Q) = 2\frac{A}{k}\int_0^{\pi} \frac{\partial G(P,Q)}{\partial n_P}(\cos m\theta_\ell)\, d\theta_\ell \qquad (8)$$

One should note that θ_p has been chosen to be zero (i.e. cos m θ_p = 1) in the above equation which can be done without any loss of generality.

Equation (3) may also be rewritten in the form

$$\int_0^{\ell}\left\{\Phi(Q)K_1(P,Q) - I_1(P,Q)V(Q)\right\} ds_\ell = 4\pi\,\Phi(P) \qquad (9)$$

As can be seen, this formulation of the problem reduces the solutions of Eqns. (1) and (3) to the evaluation of line integrals on the 2-D projections of the body (See Fig. 2.). Also, this formulation can account for tangential modes; which must, however, be solved for separately.

The theoretical method described above was checked for accuracy by employing several axisymmetric geometries including a straight duct and a jet engine inlet. The calculated radiation patterns generated by this method were compared with various "exact" solutions. These exact solutions were found by assuming that some simple sources (e.g. monopoles, dipoles, and quadrupoles) were located within the body and then calculating the normal acoustic velocity V and/or the admittance, defined as $y \equiv V/\Phi$, at points on the surface of the body. These values were then used as the boundary conditions on the surface of the body and the acoustic potential was calculated at various points in the field surrounding the body. These were then compared with the acoustic potential that the simple source would generate at each point in the field. Very good agreement was found; for 53 integration points on the body along s (See Fig. 2.) the error was always below 10% in the real and imaginary parts of Φ for nondimensional wave numbers up to ka = 10. It was also found that increasing the number of integration points generally decreased the error proportionally (e.g. using 102 points the maximum error in the acoustic potential at a field point was about 5% for the inlet at a nondimensional wave number of ka = 10.). The results and details of many such tests are presented in Ref.(3).

The Test Bodies

The integral formulation has been used in the present study to calculate the sound fields radiated from two axisymmetric bodies, a straight duct and a jet engine inlet. The theoretical and experimental configurations do not compare exactly as an accurate description of the "back side" of the experimental bodies would entail the use of too many theoretical points on the bodies. Therefore, different external terminations were given to the theoretical models in the interest of conserving computing time and computer storage space. In this connection it has been found through theoretical studies, that the exact form of the rear termination of the body has little effect on the sound field radiated in the forward half plane. Since we are only really interested in the sound field in the forward half plane, this approximation is not considered to be a major source of error in this study.

The first axisymmetric body tested was a straight duct. Below is a sketch of the theoretical model employed.

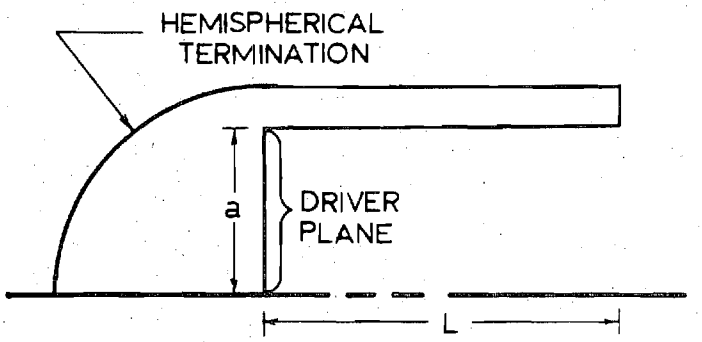

Figure 3. Theoretical Straight Duct Model.

Its L/a equals 2.110, the same as the experimental model. It will be noted that the theoretical model has a hemispherical termination which differs from the rear termination of the experimental model shown below.

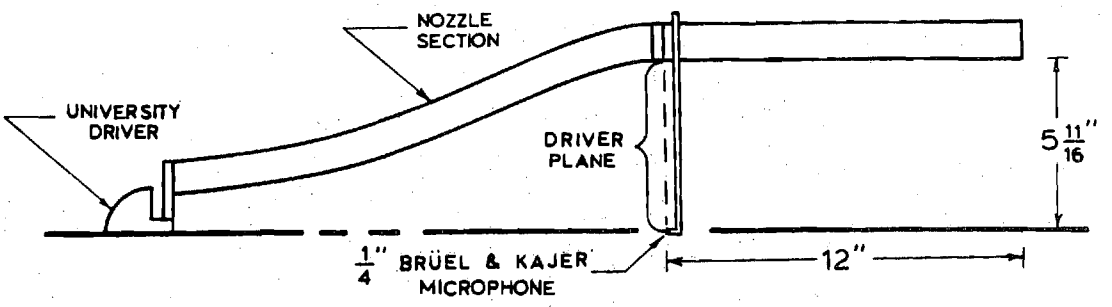

Figure 4. Experimental Straight Duct Test Configuration.

In the experimental model the driver is placed at the throat of a nozzle section, which assures that the sound waves are plane at the driver plane where a 1/4" condensor microphone is located to provide a reference pressure level in decibels. All of the tests were conducted at nondimensional wave numbers ka below the 1$\tilde{1}$ mode of the duct (i.e. $k \leq 1.84$) and thus we were assured of a plane wave at the driver plane. This has been checked out experimentally by sweeping the reference microphone radially across the duct and it has been found to be true within 1 dB in amplitude and 5° in phase (i.e. there is less than 1 dB and 5° variation between the wall and the center of the duct). In the theoretical model the existence of plane wave excitation at the driver plane is assumed.

The straight duct was tested in two configurations; that is, hard wall and lined wall configurations. The lined wall configuration consisted of 180 Helmholtz resonators (9 axial rows by 20 radial rows). A sketch of one of the resonators is shown below.

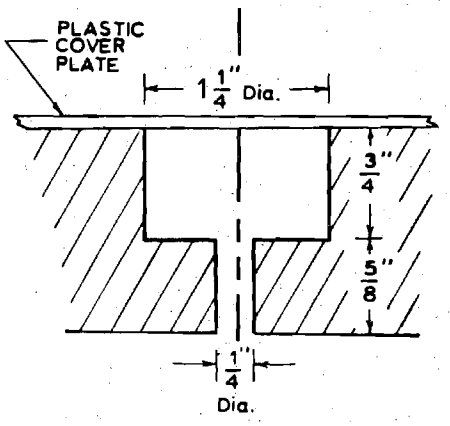

Figure 5. Helmholtz Resonator.

For the hard walled tests the small holes inside the duct were simply covered with tape.

The second axisymmetric body tested was a model of an actual engine inlet[5]. It has an L/a of 2.0. The theoretical model has a hemispherical termination similar to the one used for the straight duct. A sketch of the theoretical inlet model is presented below.

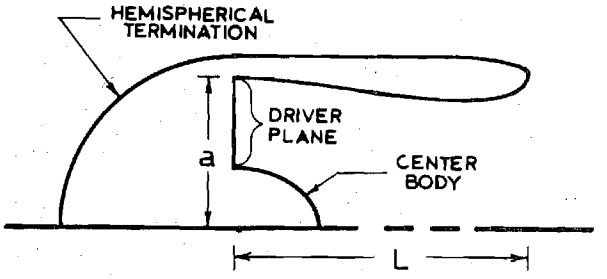

Figure 6. Theoretical Inlet Model.

In the experimental model the centerbody was held in place by 4 small wing cross-sectional struts set at 90° angles. The microphone measurement for the amplitude and phase at the driver plane was made half way between 2 of these struts. Again, the small condensor microphone was swept across the driver plane radially to check for the presence of plane wave excitation which was found to exist within the same limits as for the straight duct (i.e., less than a 1 dB change in amplitude and 5° in phase across the driver plane). A sketch of the experimental inlet model is presented below.

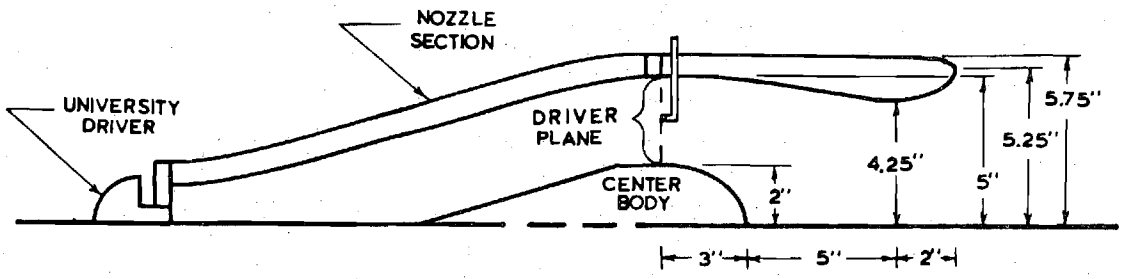

Figure 7. Experimental Inlet Test Configuration.

Again, the exact mathematical form of the curves that make up the inlet contours can be found in Reference 5.

Results

In the anachoic chamber tests conducted under this program, the field measurements were taken 40" from the center of the duct exit plane on a circular arc at 11 1/4° increments from the centerline of the duct. One-half inch B & K microphones were used in these tests for the field measurements. The anechoic chamber used in the experiments has interior dimensions of 10' x 13' x 6 1/2' high. The acoustic insulation used in the chamber is fiberglass which is approximately 2' thick. The ducts tested (i.e., the straight duct and the inlet) and the microphones used for the field measurements were 3' off the floor. A plan view of the anechoic chamber with a typical test set-up is presented below.

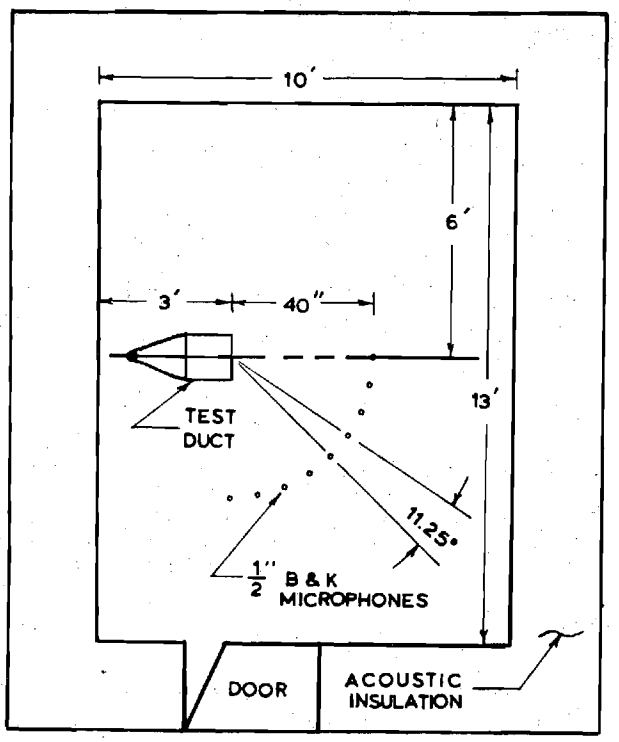

Figure 8. Anechoic Chamber (Plan View) with Test Set-Up.

Free field measurements were made in the chamber to check its "anechoicness". For the distances of interest in the chamber (i.e. up to 40" from a source) free field conditions were generally approximated to within 3 dB in amplitude and 10° in phase.

The procedure for the tests was to take the measured SPL in dB from the 1/4" B & K microphone at the driver plane and input the data into the theoretical model assuming plane wave excitation at the driver plane. Again, this was checked experimentally for each configuration and found to be generally true within 1 dB in amplitude and 5 degrees in phase. Since a plane wave was assumed, the phase was not measured at the driver plane and zero phase was assumed for this location in the theoretical model. This can be done without any loss of generality as the phase differences between the field microphones and the driver plane microphone are the quantities of interest which were measured in this program. Once the driver plane acoustic pressure was input into the theoretical model, the far field sound distribution was calculated and compared with the measured experimental data.

The computer used for these analyses was the Georgia Tech Cyber 70/74. Typical run times to calculate the distribution of the acoustic potential Φ (i.e., See Eqn. (5).) with 100 points on the theoretical body are about 6 minutes and to calculate the acoustic potential in the far field at 20 points (i.e., See Eqn. (9).) are about 1 minute. In the theoretical calculations of the surface potential on the straight duct 102 points were used while in the calculations for the inlet (See Fig. 5.) 97 points were used.

In the numerical integration of Eqns. (5) and (9) a 2 point integration formula was used in the s direction (See Fig. 2.). It should be noted, however, that an even integration formula must be used here as an odd formula would place a point in the center of the integration region which would cause the various kernel functions (i.e., See Eqns. (6)-(8).) to go to infinity when r(P,Q) goes to zero as the points P and Q coincide. In all the investigated cases a 96 point Gaussian integration formula was used in the θ direction.

Tests with the straight duct configuration with both hard and soft walls were conducted in the frequency range of 300 to 700 Hz at 50 Hz increments. Over this frequency range a reasonably plane wave could be excited at the driver plane* . Comparisons of calculated and measured data for the hard walled straight duct configuration are

* In this study the lower frequency limit was imposed by the limitations of the University driver.

presented in Fig. 9 for 550 Hz. The SPL results at this frequency are representative of those at all other frequencies while the phase results are the worst at this frequency. The probable reason for this is that 550 Hz is very close to the tuning frequency of the liner, which was calculated to be around 558 Hz under these test conditions and the tape used to close off the liner holes for the hard walled tests was not 100 percent effective. The average absolute errors for the amplitude in dB and for the phase in degrees are presented in Table I for all of the tests run.

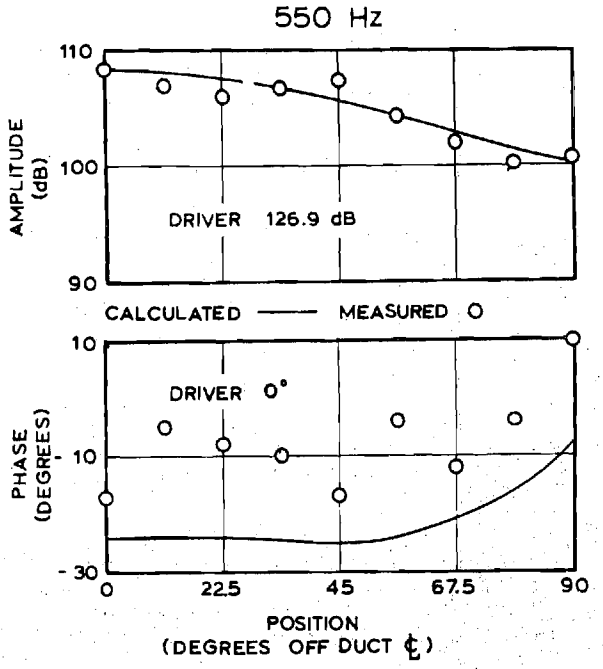

Figure 9. Acoustic Radiation 40" from the Hard Walled Straight Duct.

To predict the sound field radiated by the lined, straight wall duct the admittance at the wall is required. In this case available liner theory[7] was used to predict the admittance of the Helmholtz resonator array. For the particular resonators used (See Fig. 5.) in this study the resonant frequency of the array, f_o, was calculated to be around 558 Hz and the specific impedance of the liner $Z = \Theta - i\chi$ was found to be given by:

$$\Theta = 0.01398\sqrt{f}$$

$$\chi = 10.186\left(\frac{f}{f_c} - \frac{f_c}{f}\right) \qquad (10)$$

Comparisons of experimental and calculated far field pressures for the lined, straight wall duct are presented in Fig. 10 at a frequency of 500 Hz. These results are typical of those obtained at all but one of the other frequencies tested. At 550 Hz, which is very close to the calculated resonant frequency of the liner, the results show significantly more error (See Table I.). Since the calculated results were lower than those measured it was assumed that the liner theory results predicted the effectiveness of the liner to be higher than it actually was in practice. To see if this was actually the case a set of systematic computer runs were made in which the effectiveness of the liner (i.e., its admittance) was reduced.

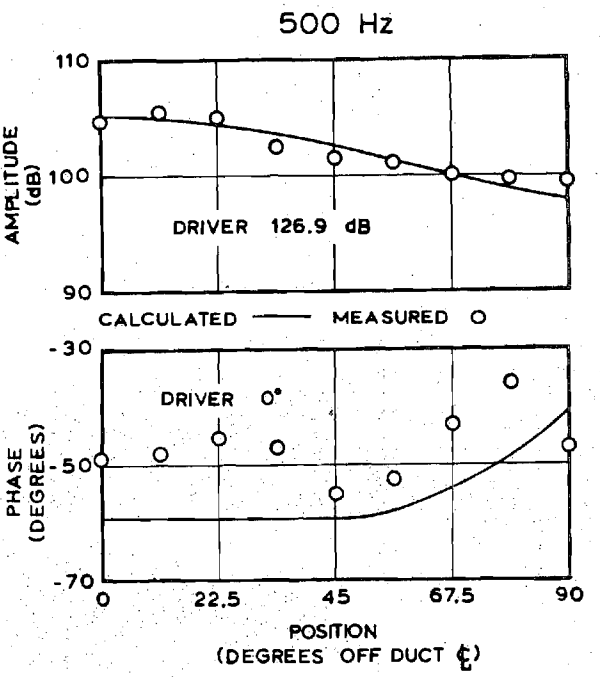

Figure 10. Acoustic Radiation 40" from the Soft Walled Straight Duct.

It was found that if the predicted real part of the admittance was taken to be 35 percent effective and the imaginary part of the admittance was taken to be 65 percent effective (i.e. $y = - 0.13 - i\ 0.28$ at 550 Hz) than the results from the theoretical calculations were significantly closer to the experimentally measured data. The average absolute errors for the amplitude in dB and for the phase in degrees are now 2.51 dB and 5.00 degrees respectively as compared to the much larger errors incurred using the admittance values predicted by the liner theory (See Table I.).

Tests for the inlet configuration were also conducted over the frequency range 300 - 700 Hz at 50 Hz increments. Since the reference lengths, a, are slightly different (See Figs. 3,4,6 and 7.) the nondimensional wave numbers ka are different. Comparisons of theoretical and experimental data are presented in Fig. 11 for the inlet configuration at 600 Hz. These results are representative of those at other frequencies.

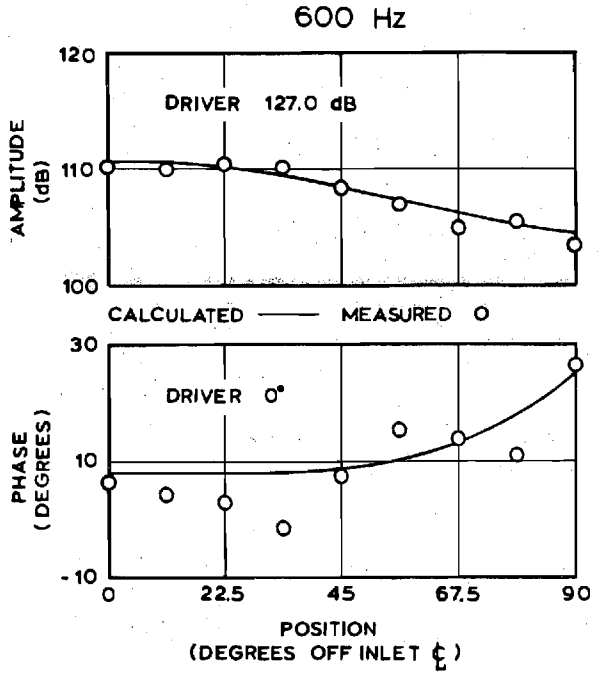

Figure 11. Acoustic Radiation 40" from the Inlet.

Discussion of Results

The causes for the errors appearing in the comparisons of the last section will be briefly discussed herein. First, there are the obvious experimental errors caused by microphone amplifier drift, temperature changes in the anechoic chamber and microphone placement in the chamber. These errors can be estimated as identical tests were run on different days, the microphones were calibrated three times during the course of each test, and the microphones were moved and reset during each test as there are 9 positions in the field and only 5 microphones were used in each test. Comparing test results and calibrations, these errors are estimated as being of the order of 0.5 dB in amplitude and 5 degrees in phase. Another source of experimental error is the anechoic chamber itself which, as stated before, can account for up to 3 dB errors in amplitude and 10° errors in phase. A more subtle source of error in the lined duct tests is the liner itself. It was found that by changing the dimensions of the Helmholtz resonators by as little as 0.0005 inches (i.e. common machining errors) the resonant frequency calculated for the liner changed by as much as 1.5 Hz which is significant for this type of liner near resonance due to its highly peaked absorption curve. A sample calculation was run at 550 Hz with this change and the calculated results changed by about 3 dB in amplitude and 5 degrees in phase. Another source of possible error for this particular case is obviously the imperfection of the liner theory itself; the determination of the errors caused by its shortcomings are, however, beyond our current capabilities.

The computer programs also introduce some errors which are estimated to be about 1 percent by comparing these computer results with exact solutions for similar geometries and wave numbers. Although these errors are insignificant when evaluated in dB, they can be as high as 5 degrees in phase. Another source of error is the assumption of a plane wave at the driver plane; the effect of this error or the results in the far field cannot, however, be easily estimated. Other sources of error include the differences between the experimental and theoretical geometries which include not only the different terminations on the back side of the bodies but also the stand required to hold up the experimental set-up in the anechoic chamber. The errors caused by these differences are hopefully small.

Freq. Hz		300	350	400	450	500	550	600	650	700
Hard Walled Straight Duct	dB	0.96	0.95	0.66	0.70	0.71	0.78	0.92	0.67	1.02
	Deg.	3.83	5.56	5.89	4.61	7.44	13.78	4.33	7.72	7.83
Soft Walled Straight Duct	dB	1.06	1.96	0.82	0.63	0.74	15.71	1.61	0.42	1.19
	Deg.	4.67	4.78	9.28	3.67	9.33	88.89	8.11	5.89	6.61
Inlet	dB	1.18	0.72	0.61	1.08	0.69	0.63	0.61	0.38	1.07
	Deg.	3.17	6.39	3.83	10.22	5.00	6.22	4.00	4.50	5.00

Table I. Average Absolute Errors.

Conclusions

Acoustic measurements were made of the sound field radiated from a straight duct with both acoustically hard and soft walls and a jet engine inlet. These measurements were then compared with the results of an integral representation of the solutions of the Helmholtz equation and good agreement between the theoretical and experimental results was observed. This indicates that the integral equations used and the techniques employed for solving them are good approximations to the actual acoustic behavior of arbitrarily shaped axisymmetric ducts radiating into a free space. This is significant in that most theories can not adequately model the coupling between the acoustic fields inside and outside a duct. Thus, this technique can be used with confidence to efficiently predict the sound field radiated from complex axisymmetric geometries.

References

1. Bell, W. A., Meyer, W. L., and Zinn, B. T., "Predicting the Acoustics of Arbitrarily Shaped Bodies Using an Integral Approach," AIAA Journal Vol. 15, No. 6, June 1977, pp. 813-820.

2. Meyer, W. L., Bell, W. A., Stallybrass, M. P. and Zinn, B. T., "Boundary Integral Solutions of Three Dimensional Acoustic Radiation Problems," Journal of Sound and Vibration, Vol. 59, No. 2, pp. 245-262, July 1978.

3. Meyer, W. L., Bell, W. A., Stallybrass, M. P., and Zinn, B. T., "Prediction of the Sound Field Radiated From Axisymmetric Surfaces," Journal of the Acoustical Society of America, Vol. 65, No. 3, pp. 631-638, March 1979.

4. Meyer, W. L., Bell, W. A., and Zinn, B. T., "Sound Radiation from Finite Length Axisymmetric Ducts and Engine Inlets," AIAA Paper No. 79-0675, presented at the AIAA 5th Aeroacoustics Conference, Seattle, Washington, March 12-14, 1979.

5. Miller, B. A., Dastoli, B. J., and Wesoky, H. L., "Effect of Entry-Lip Design on Aerodynamics and Acoustics of High-Throat-Mach-Number Inlets for the Quiet, Clean, Short-Haul Experimental Engine," NASA TM X-3222, May 1975.

6. Burton, A. J., "The Solution of Helmholtz' Equation in Exterior Domains Using Integral Equations," NPL Report NAC 30, National Physical Laboratory, Teddington, Middlesex, January 1973.

7. Garrison, G. D., "A Study of the Suppression of Combustion Oscillations with Mechanical Damping Devices," Phase II Summary Report, Pratt & Whitney Aircraft Co., PWA FR-1922, July 15, 1966.